CHEMISTRY
A EUROPEAN JOURNAL

DOI: 10.1002/chem.200801815

A Synthetic Method for Transition-Metal Chalcogenide Nanocrystals

Ding-Sheng Wang, Wen Zheng, Chen-Hui Hao, Qing Peng, and Ya-Dong Li*[a]

Abstract: In this paper, we prepared a series of chalcogenide semiconductor nanocrystals in controllable shape and size via a facile wet route using metal nitrates and sulfur or selenium powder as precursors and octadecylamine (ODA) as solvent. The as-obtained chalcogenides included CdS, MnS, Ag_2S, PbS, $Cu_{1.8}S$, Bi_2S_3, ZnS, $Zn_xCd_{1-x}S$, as well as Ag_2Se, $Cu_{2-x}Se$, CdSe, MnSe. Furthermore, these cyclohexane-soluble monodisperse nanocrystals were assembled to water-soluble colloidal spheres and the adjustment of assembly orderliness has been achieved by controlling the experimental parameters. The general synthesis and assembly of chalcogenide semiconductors provide ideal building blocks for various potential applications.

Keywords: chalcogens · colloids · nanostructures · semiconductors · transition metals

Introduction

During the past decades, chalcogenide semiconductor nanocrystals (metal sulfides and selenides) have attracted broad attention due to their unique shape- and size-dependent physical and chemical properties that differ drastically from their bulk counterparts.[1–4] These nanocrystals find potential applications in various fields such as solar cells, electrical, optical and magnetic devices, biological labeling and diagnostics, hydrodesulfurization and hydrogenation catalysts.[5–11] For example, multifunctional nanoparticle probes based on semiconductor quantum dots (CdSe–ZnS core–shell QDs) were developed for cancer targeting and imaging in living animals by the Nie group;[10a] Gothelf et al. also reported a metal sulfide nanoparticle-based (CdS, ZnS, and PbS NPs) electrochemical detection method that provided detection capabilities down to 100 attomol for target DNA.[10b] Thus, synthesis of chalcogenide semiconductor nanocrystals in controllable shape and size is of great significance for modern science and technology.

The methods for chalcogenides include gas-phase syntheses and solution-based strategies.[12–26] The former usually requires high temperature and pressure, and the procedure is complicated. Comparatively, the solution-based method is much milder and more convenient. As early as 1993, Bawendi et al. successfully synthesized high-quality nearly monodisperse CdSe semiconductor QDs using Me_2Cd and TOPSe as precursors and trioctylphosphine (TOP)/trioctylphosphine oxide (TOPO) as solvents, which opened a simple synthetic route to the production of semiconductor nanocrystals.[27] In the following years, many groups continuously developed the method. In 2000, it was first observed by Peng et al. that shape control of CdSe nanocrystals could be achieved by changing the surfactants from pure TOPO to TOPO/hexylphosphonic acid (HPA) and rod-like CdSe with aspect ratios as large as ten to one was prepared.[28] In 2003, the Hyeon group reported on the synthesis of semiconductor nanocrystals of PbS, ZnS, CdS, and MnS using metal/oleylamine complexes as precursors and their shape and size could be controlled by adjusting the experimental conditions.[29] Furthermore, ternary chalcogenides were also synthesized through a modified approach by Qian et al. in 2007 and monodisperse pyramidal $CuInS_2$ and rectangular $AgInS_2$ nanocrystals were obtained using HDA as the capping reagent and anisole as the solvent.[30] However, from a scientific perspective, supply of more experimental data is still needed to understand the growth kinetics and structural polymorphism in nanocrystals; from an industrial perspective, exploration of more convenient synthetic strategy is still needed to meet the demand for future applications of chalcogenide semiconductors.

Very recently, we developed a general strategy for the direct thermal decomposition of metal nitrates in ODA to synthesize various metal oxide nanocrystals.[31] If we would introduce sulfur or selenium powder into the above system,

[a] D.-S. Wang, W. Zheng, C.-H. Hao, Dr. Q. Peng, Prof. Dr. Y.-D. Li
Department of Chemistry
Tsinghua University
Beijing, 100084 (PR China)
Fax: (+86) 10-62788765
E-mail: ydli@mail.tsinghua.edu.cn

metal sulfide and selenide nanocrystals would be obtained instead.[32–34] Herein, we will describe the preparation of various chalcogenide semiconductors, such as CdS, MnS, Ag_2S, PbS, $Cu_{1.8}S$, Bi_2S_3, ZnS, $Zn_xCd_{1-x}S$, Ag_2Se, $Cu_{2-x}Se$, CdSe, and MnSe. CdS and MnS nanocrystals are used as examples to show how their morphologies can be controlled by adjusting the experimental parameters. On the other hand, assembly of nanocrystal building blocks is of key importance for the construction of functional architectures and integrating nanoscale devices. Therefore, we also present general assembly of as-obtained chalcogenide nanocrystals which can even control the assembly order.

Results and Discussion

CdS nanocrystals: In our synthesis of CdS nanocrystals, we employed cadmium nitrate and sulfur powder as precursors and ODA as solvent. Under optimized reaction conditions, high-quality nearly monodisperse CdS semiconductors could be produced effectively. Their shape and size were mainly affected by the concentration of the sulfur powder and reaction temperature. Transmission electron microscope (TEM) images of as-obtained different CdS nanocrystals under controlled conditions are shown in Figure 1. At high temperatures such as 200 °C, we could obtain CdS nanorectangles with average length of 25 nm and width of 12 nm (Figure 1A) when a sulfur amount of 0.05 g was used (0.1 g of $Cd(NO_3)_2{\cdot}4H_2O$ and 10 mL of ODA). When we reduced the sulfur amount to 0.01 g, CdS nanobullets with an average size of 10 nm were obtained instead (Figure 1B and D), which was the first synthesis of the novel bullet-like CdS nanocrystals. Powder X-ray diffraction (XRD) measurements were carried out to determine their structure and composition, and the results is shown in Figure 1C. All diffraction peaks in the pattern can be assigned to the wurtzite-phase CdS (JCPDS 41-1049). At 120 °C, the results were obviously different. CdS nanoparticles with a small size of about 5 nm were obtained when 0.01 g sulfur were used (Figure 1E). Figure 1F displays as-prepared CdS nanocrystals with an increased sulfur amount of 0.05 g; the nanocrystals show tripod-like morphology with three arms of about 50 nm in length and about 15 nm in diameter.

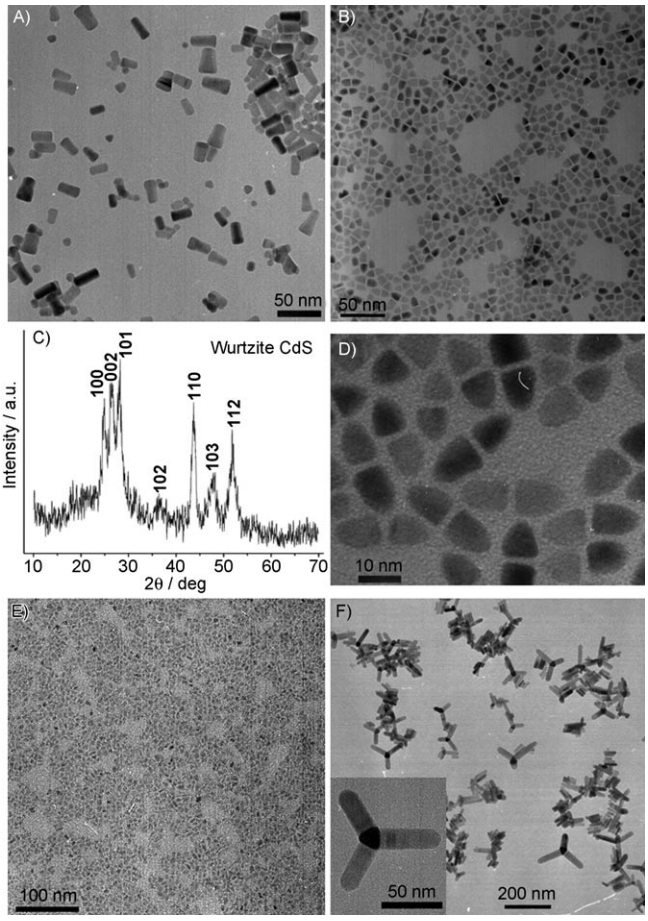

Figure 1. TEM images of A) CdS nanorectangles, E) CdS nanoparticles, and F) CdS nanotripods; B and D) TEM images of CdS nanobullets at different magnifications; C) XRD pattern of CdS nanobullets.

MnS nanocrystals: Structure- and morphology-controlled MnS nanocrystals were synthesized with a similar way. It is well known that MnS crystallizes in one of three polymorphs: the thermodynamically stable green α phase MnS with rock-salt-type structure, and two pink metastable tetrahedral structures, β phase MnS (sphalerite type) and γ phase MnS (wurtzite type).[35] In our synthesis, the sulfur dosage was the key parameter to control the phase of products: α-MnS was prepared with a high concentration of sulfur powder while γ-MnS was obtained with low sulfur content. The phase identification was performed using XRD measurements. As shown in Figure 2A, the series of Bragg reflections in the pattern correspond to the cubic unit cell of α-MnS with lattice parameter $a = 5.228$ Å (JCPDS 06-0518). It can also be observed from Figure 2B that all characteristic peaks in the pattern can be readily indexed to the wurtzite-phase γ-MnS (JCPDS 40-1289). Figure 2C and D show TEM images of as-synthesized α-MnS and γ-MnS, respectively. The α-MnS nanocrystals are hexagon-like particles with an average size of 50 nm and γ-MnS nanocrystals exhibit rod-like morphology with a diameter of about 50 nm and length up to hundreds of nanometers. We can also see from the inset of Figure 2D that tetrapod-like γ-MnS coexists in the products.

Other metal sulfide nanocrystals: A series of metal sulfide semiconductors can be prepared with a method similar to that for CdS and MnS nanocrystals. Figure 3A shows as-obtained Ag_2S nanoparticles with an average diameter of 15 nm. Due to their uniform size, these particles can assemble to hexagonal-packed arrays on carbon-covered-copper TEM microgrid. Figure 3B shows as-obtained PbS nanocrystals. Viewed in-plane, the nanocrystals are square in shape with dimension of about 10 nm. They can also self-assemble into ordered 2D arrays on the copper grid. Figure 3E and F display as-obtained ZnS nanoparticles and Bi_2S_3 nanorods,

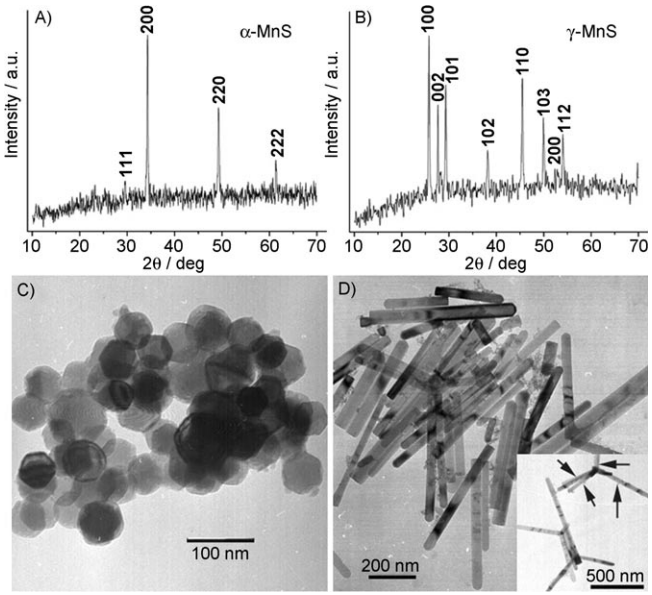

Figure 2. A and B) XRD patterns of α-MnS and γ-MnS nanocrystals respectively; C and D) TEM images of α-MnS and γ-MnS nanocrystals, respectively.

respectively. ZnS particles have an average size of 10 nm and a tendency to form to elongated crystals. The Bi_2S_3 rods have diameters in the range of 15–30 nm and lengths up to hundreds of nanometers. Figure 3D shows as-obtained $Cu_{1.8}S$ nanocrystals with an unusual composition, which was determined by XRD measurements. From the result shown in Figure 3C, we can see that the series of Bragg reflections in the pattern correspond to the orthorhombic-phase $Cu_{1.8}S$ (JCPDS 75-2241). These nanocrystals exhibit disk-like morphology with an average diameter of 10 nm and some of the nanodisks can self-assemble face-to-face on copper grid.

Metal selenide nanocrystals: When we used selenium powder instead of sulfur powder, the corresponding metal selenide semiconductors could be synthesized. Figure 4A shows as-obtained Ag_2Se nanoparticles with an average diameter of 10 nm. Because of the much lower chemical reactivity of selenium compared with sulfur, the monodispersity of Ag_2Se nanoparticles is not as good as Ag_2S. CdSe nanoparticles with an average size of only 5 nm (Figure 4E) and MnSe nanoparticles with dimension of about 200 nm (Figure 4F) could also be obtained via this simple route. Similar to $Cu_{1.8}S$, the as-obtained $Cu_{2-x}Se$ nanocrystals also have un-

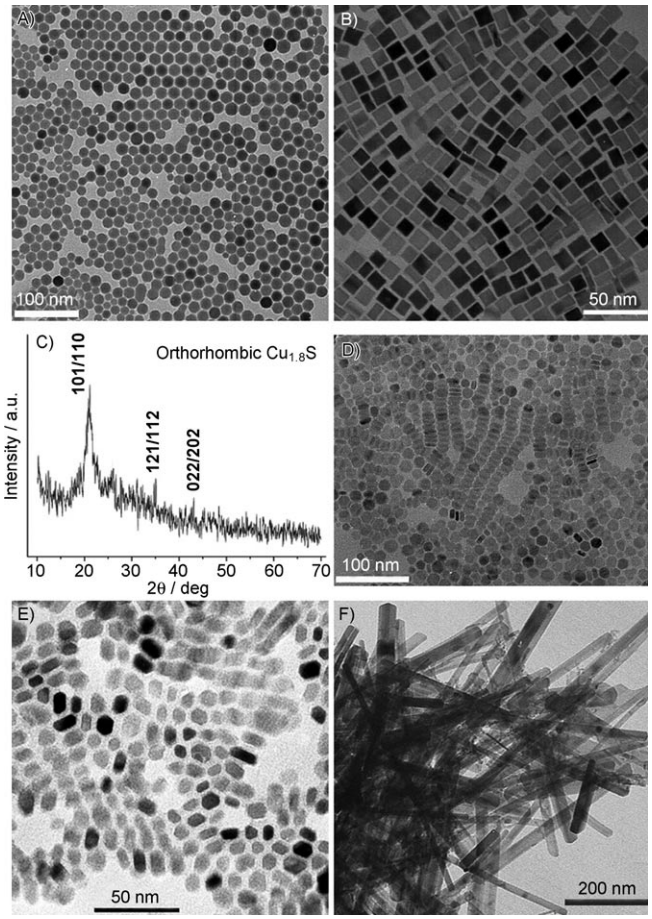

Figure 3. TEM images of A) Ag_2S nanoparticles, B) PbS nanocubes, D) $Cu_{1.8}S$ nanodisks, E) ZnS nanoparticles, and F) Bi_2S_3 nanorods; C) XRD pattern of $Cu_{1.8}S$ nanodisks.

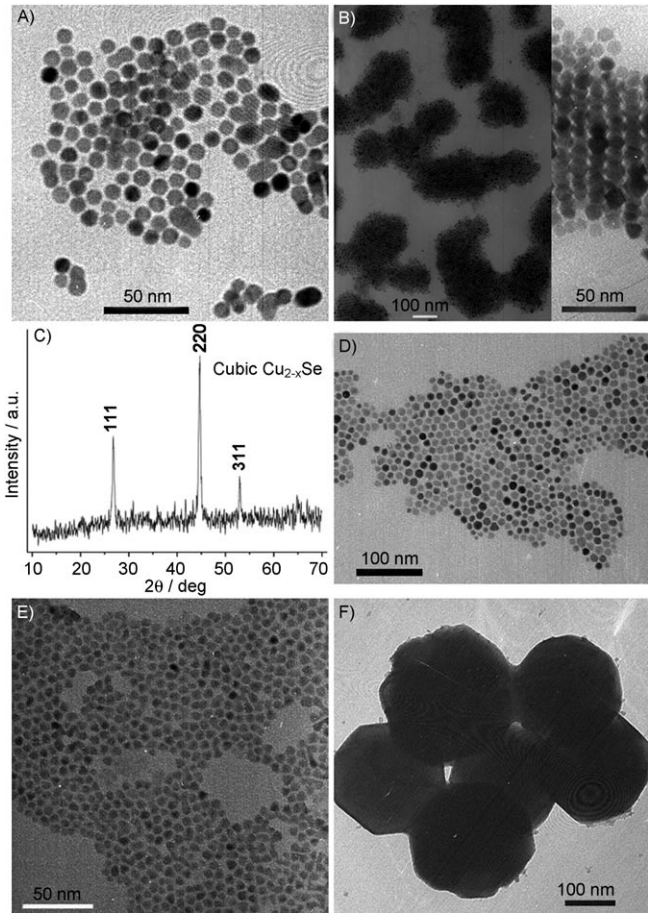

Figure 4. TEM images of A) Ag_2Se nanoparticles, D) $Cu_{2-x}Se$ nanoparticles, E) CdSe nanoparticles, and F) MnSe nanoparticles; B) TEM image of $Cu_{2-x}Se$ superlattices; C) XRD pattern of $Cu_{2-x}Se$ nanocrystals.

usual composition. It can be observed from the XRD pattern in Figure 4C that all characteristic peaks match exactly with the standard JCPDS card 06-0680 of cubic-phase $Cu_{2-x}Se$. Figure 4D shows their particle morphology with an average size of 10 nm. Under certain reaction conditions, they can form superlattices by spontaneous alignment of $Cu_{2-x}Se$ nanoparticles (Figure 4B). From the TEM image at larger magnification (Figure 4B, inset), 0D $Cu_{2-x}Se$ particles have a tendency to evolve to 1D wires through oriented attachment of nanocrystal building blocks.

$Zn_xCd_{1-x}S$ semiconductors and corresponding optical properties: When we started with a combination of zinc nitrate and cadmium nitrate, $Zn_xCd_{1-x}S$ nanocrystals were prepared. The stoichiometry x could be adjusted by controlling the molar ratio of different metal nitrates. We synthesized a series of $Zn_xCd_{1-x}S$ ($x=1$, 0.6, 0.4, 0) semiconductors and studied their optical properties. There is no obvious difference for the particle shape and distribution in the $Zn_xCd_{1-x}S$ series. They are all particles with an average size of 10 nm similar to ZnS (Figure 3E). Figure 5A shows the visible absorption spectra of as-obtained samples dispersed in cyclohexane. From the visual images of these transparent solutions (Figure 5A, inset), we observed that the color changes from white to yellow with the increase of the Cd^{2+} content. Under 365 nm excitation, the semiconductors exhibited excellent luminescent properties and their fluorescence spectra are presented in Figure 5B. The multicolor luminescence photos of the semiconductors (Figure 5B, inset) show strong emissions from blue to red, indicating that the band gap of semiconductor nanocrystals can be modulated by forming the nanocrystal alloys.

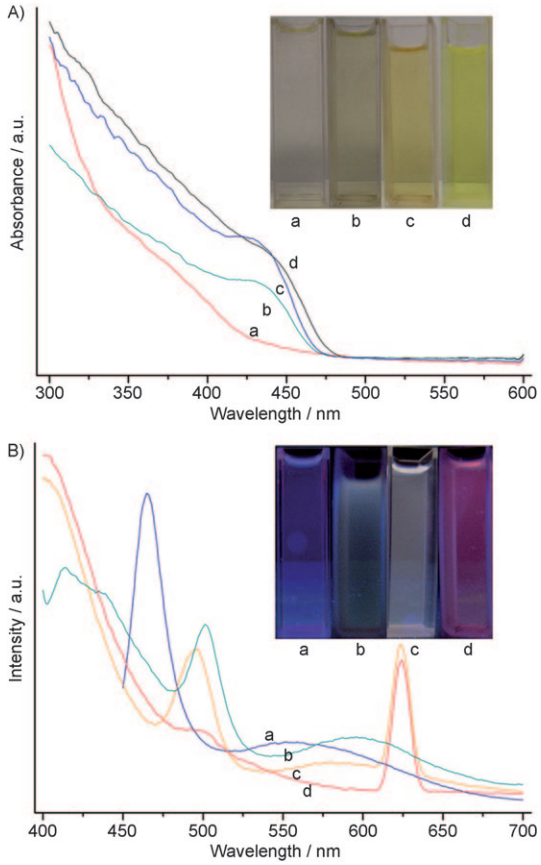

Figure 5. A) Visible absorption spectra and visual images of as-obtained $Zn_xCd_{1-x}S$ ($x=1$ (a), 0.6 (b), 0.4 (c), 0 (d)) semiconductors; B) Fluorescence spectra and luminescence photos of $Zn_xCd_{1-x}S$ ($x=1$ (a), 0.6 (b), 0.4 (c), 0 (d)) semiconductors.

Furthermore, more complex $Zn_xCd_{1-x}S_ySe_{1-y}$ nanocrystals could also be obtained when we introduced zinc nitrate, cadmium nitrate, sulfur and selenium into the reaction system. By controlling the values of x and y, we can adjust the band gap of this series of semiconductors as we wish. Thus, this simple route provides a very general method for chalcogenide semiconductors. Most of the metal sulfide and selenide nanocrystals as well as ternary semiconductors can be synthesized via this strategy. Other general precursors such as metal chlorides can also be employed as reagents instead of metal nitrates. Therefore this route can achieve low-cost and large-scale preparation of semiconductor nanocrystals.

Assembly of semiconductor nanocrystals: The as-prepared chalcogenide nanocrystals with controllable shape and size provide ideal building blocks for constructing complex nanostructures and fabricating functional semiconductor materials. We employ a surfactant-assisted bottom-up self-assembly approach to design 3D colloidal spheres from 0D nanocrystals.[36] $Cu_{1.8}S$ was taken as an example to show this assembly process. Figure 6 displays TEM images of $Cu_{1.8}S$ colloidal spheres and the assembly results were greatly affected by experimental conditions. When ultrasonic treatment was employed during the process, we could obtain nearly monodisperse colloidal spheres (Figure 6A). From the image at high magnification shown in Figure 6B, we can see clearly that these spheres are composed of disordered $Cu_{1.8}S$ nanodisks. When the reaction mixture was stirred, polydisperse colloidal ellipsoids were obtained instead (Figure 6C). Their high-magnification images (Figure 6D and E) obviously show that $Cu_{1.8}S$ nanodisks in the ellipsoids are highly ordered. Moreover, the high-resolution transmission electron microscope (HRTEM) image shown in Figure 6F demonstrates that the $Cu_{1.8}S$ building blocks are well crystallized.

Based on the above experimental results, we assume that the means of treatment with original two-phase system is the key parameter to control the assembly order and present a proposed mechanism for this process with a schematic diagram in Figure 7. First, we designed a two-phase system, that is, oil phase which contained pre-prepared well-dispersed $Cu_{1.8}S$ nanodisks stabilized by ODA and water phase containing cetyltrimethylammonium bromide (CTAB). Thus, we obtained a stable oil-in-water microemulsion system via ultrasonic or stirring treatment. The difference between the two means was the different energy they offered. Enough energy could be provided by the ultrasonic treatment to form uniform spherical oil droplets. On the other hand, $Cu_{1.8}S$ nanodisks encapsulated in the droplets would present random movement and collision due to the

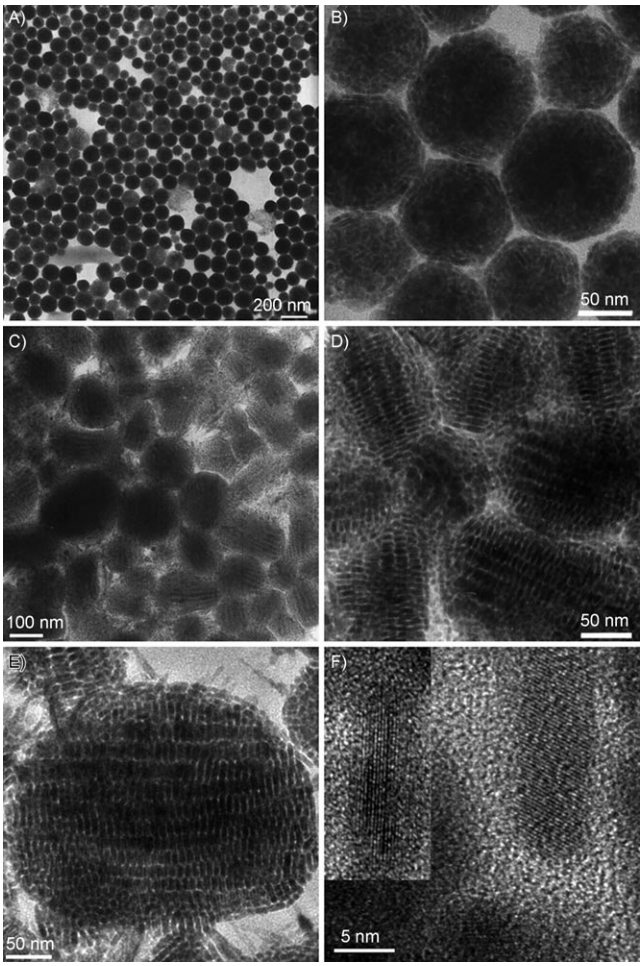

Figure 6. A and B) TEM images of $Cu_{1.8}S$ colloidal spheres at different magnifications; C, D and E) TEM images of $Cu_{1.8}S$ colloidal ellipsoids at different magnifications; F) HRTEM image of $Cu_{1.8}S$ nanodisks.

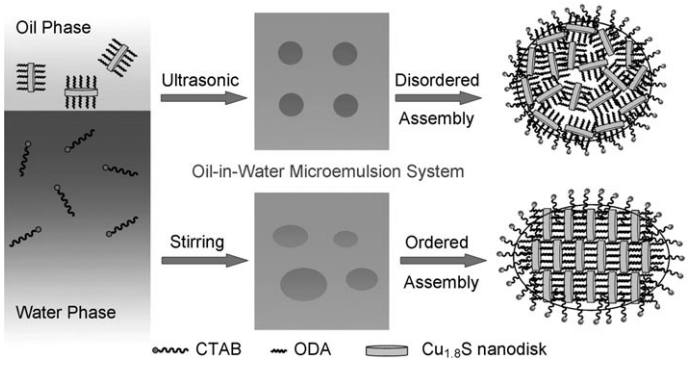

Figure 7. Scheme of $Cu_{1.8}S$ nanodisk assembly processes.

high-energy environment. Therefore disordered assembly occurred. However, upon mechanical stirring, elliptical oil droplets formed and their sizes could not be uniform. Because the energy provided by stirring was not enough to destroy the hydrophobic van der Waals interactions between surfactants located outside surface of $Cu_{1.8}S$ nanodisks, the building blocks confined in the droplets would self-assemble to well-ordered superstructures.

Conclusion

In summary, a facile one-pot synthetic procedure for the shape- and size-controlled preparation of chalcogenide semiconductor nanocrystals has been successfully developed in the present study. Nontoxic inorganic salts and inexpensive sulfur or selenium powder were employed as reagents. This simple and general strategy offered the possibility of low-cost and large-scale production of high-quality semiconductors. On the other hand, these semiconductor nanocrystals could be used as ideal building blocks to construct more complex architectures. The as-assembled 3D colloidal semiconductors provided controllable structures, hydrophilic surface and various properties, which promises their potential applications in various fields such as solar cells and biochemistry.

Experimental Section

Materials: All reagents used in this work, including various kinds of inorganic salts, sulfur and selenium powder, ODA, ethanol, and cyclohexane were of A.R. grade from the Beijing Chemical Factory, China.

Synthesis: A typical procedure for the preparation of chalcogenide semiconductor nanocrystals such as CdS nanobullets was described as follows: $Cd(NO_3)_2{\cdot}4H_2O$ (0.1 g) and sulfur powder (0.01 g) were added into ODA (10 mL) at 200 °C. After 10 min of magnetically stirring, the system was maintained at this temperature for further growth and crystallization for 6–24 h. The final products were collected at the bottom of the beaker. The CdS nanobullets were washed several times with ethanol, and then dispersed in non-polar solvent such as cyclohexane. The experimental parameters of sulfur concentration and reaction temperature were adjusted to obtain shape- and size-controlled CdS nanocrystals such as nanorectangles (0.05 g S, 200 °C), nanoparticles (0.01 g S, 120 °C), and nanotripods (0.05 g S, 120 °C). The other chalcogenide semiconductors could be synthesized based on the similar process and the applied precursors were replaced by corresponding inorganic salts.

Assembly: A typical assembly process for $Cu_{1.8}S$ nanodisks was described as follows: CTAB (0.3 g) was dissolved into deionized water (100 mL), and then $Cu_{1.8}S$ nanodisk solution (10 mL, $\approx$10 mg mL^{-1}, the solvent is cyclohexane) was added. The as-obtained system was emulsified by ultrasonic or stirring treatment at room temperature for 1 h. After that, they were heated to 80 °C and stirred for another 1 h to evaporate the cyclohexane. The $Cu_{1.8}S$ colloidal spheres or ellipsoids were obtained by centrifuging and washing with water.

Characterization: The powder XRD patterns were recorded with a Bruker D8-advance X-ray powder diffractometer with $Cu_{K\alpha}$ radiation ($\lambda = 1.5406$ Å), keeping the operation voltage and current at 40 kV and 40 mA, respectively. The 2θ range used was from 10 to 70° in steps of 0.02° with a count time of 2 s. The size and morphology of as-synthesized samples were determined by using Hitachi Model H-800 TEM and JEOL-2010F HRTEM. Samples were prepared by placing a drop of a dilute cyclohexane dispersion of the nanocrystals on the surface of a copper grid. The visible absorption spectra were performed on Shimadzu UV-2100S from 300 to 600 nm and the fluorescence spectra were recorded by using a Fluorescence Spectrophotometer (Hitachi F-4500).

Acknowledgement

This work was supported by NSFC (90606006), the State Key Project of Fundamental Research for Nanoscience and Nanotechnology (2006CB932300), the Key grant Project of Chinese Ministry of Education (NO.306020), and National Undergraduate Innovation Training Project.

[1] A. P. Alivisatos, *Science* **1996**, *271*, 933.
[2] C. B. Murray, C. R. Kagan, M. G. Bawendi, *Annu. Rev. Mater. Sci.* **2000**, *30*, 545.
[3] a) Y. Huang, X. F. Duan, Y. Cui, L. J. Lauhon, K. H. Kim, C. M. Lieber, *Science* **2001**, *294*, 1313. b) Y. Xia, P. Yang, Y. Sun, Y. Wu, B. Mayers, B. Gates, Y. Yin, F. Kim, H. Yan, *Adv. Mater.* **2003**, *15*, 353.
[4] R. Viswanatha, D. M. Battaglia, M. E. Curtis, T. D. Mishima, M. B. Johnson, X. G. Peng, *Nano Res.* **2008**, *1*, 138.
[5] Y. Cui, C. M. Lieber, *Science* **2001**, *291*, 851.
[6] W. U. Huynh, J. J. Dittmer, A. P. Alivisatos, *Science* **2002**, *295*, 2425.
[7] N. Tessler, V. Medvedev, M. Kazes, S. H. Kan, U. Banin, *Science* **2002**, *295*, 1506.
[8] V. C. Sundar, H. J. Eisler, M. G. Bawendi, *Adv. Mater.* **2002**, *14*, 739.
[9] J. C. Johnson, H. J. Choi, K. P. Knutsen, R. D. Schaller, P. D. Yang, R. J. Saykally, *Nat. Mater.* **2002**, *1*, 106.
[10] a) X. Gao, Y. Cui, R. M. Levenson, L. W. K. Chung, S. Nie, *Nat. Biotechnol.* **2004**, *22*, 969. b) J. A. Hansen, R. Mukhopadhyay, J. Ø. Hansen, K. V. Gothelf, *J. Am. Chem. Soc.* **2006**, *128*, 3860.
[11] M. S. Wang, I. Kaplan-Ashiri, X. L. Wei, R. Rosentsveig, H. D. Wagner, R. Tenne, L. M. Peng, *Nano Res.* **2008**, *1*, 22.
[12] B. Gates, Y. Wu, Y. Yin, P. Yang, Y. Xia, *J. Am. Chem. Soc.* **2001**, *123*, 11500.
[13] Y. W. Jun, Y. Y. Jung, J. Cheon, *J. Am. Chem. Soc.* **2002**, *124*, 615.
[14] L. Manna, D. J. Milliron, A. Meisel, E. C. Scher, A. P. Alivisatos, *Nat. Mater.* **2003**, *2*, 382.
[15] Y. Zhao, Y. Zhang, H. Zhu, G. C. Hadjipanayis, J. Q. Xiao, *J. Am. Chem. Soc.* **2004**, *126*, 6874.
[16] Z. Liu, J. Liang, S. Li, S. Peng, Y. Qian, *Chem. Eur. J.* **2004**, *10*, 634.
[17] S. Santra, H. Yang, P. H. Holloway, J. T. Stanley, R. A. Mericle, *J. Am. Chem. Soc.* **2005**, *127*, 1656.
[18] J. P. Ge, S. Xu, J. Zhuang, X. Wang, Q. Peng, Y. D. Li, *Inorg. Chem.* **2006**, *45*, 4922.
[19] F. M. Michel, M. A. A. Schoonen, X. V. Zhang, S. T. Martin, J. B. Parise, *Chem. Mater.* **2006**, *18*, 1726.
[20] X. Wang, J. Zhuang, Q. Peng, Y. D. Li, *Langmuir* **2006**, *22*, 7364.
[21] J. J. Vittal, M. T. Ng, *Acc. Chem. Res.* **2006**, *39*, 869.
[22] J. Xu, J. P. Ge, Y. D. Li, *J. Phys. Chem. B* **2006**, *110*, 2497.
[23] M. Fardy, A. I. Hochbaum, J. Goldberger, M. M. Zhang, P. Yang, *Adv. Mater.* **2007**, *19*, 3047.
[24] a) D. J. Milliron, M. A. Caldwell, H. S. P. Wong, *Nano Lett.* **2007**, *7*, 3504. b) J. Sun, W. E. Buhro, *Angew. Chem.* **2008**, *120*, 3259; *Angew. Chem. Int. Ed.* **2008**, *47*, 3215.
[25] a) A. B. Hungria, B. H. Juárez, C. Klinke, H. Weller, P. A. Midgley, *Nano Res.* **2008**, *1*, 89. b) R. Kitaura, D. Ogawa, K. Kobayashi, T. Saito, S. Ohshima, T. Nakamura, H. Yoshikawa, K. Awaga, H. Shinohara, *Nano Res.* **2008**, *1*, 152.
[26] P. Li, L. Y. Wang, L. Wang, Y. D. Li, *Chem. Eur. J.* **2008**, *14*, 5951.
[27] C. B. Murray, D. J. Norris, M. G. Bawendi, *J. Am. Chem. Soc.* **1993**, *115*, 8706.
[28] X. G. Peng, L. Manna, W. D. Yang, J. Wickham, E. Scher, A. Kadavanich, A. P. Alivisatos, *Nature* **2000**, *404*, 59.
[29] J. Joo, H. B. Na, T. Yu, J. H. Yu, Y. W. Kim, F. Wu, J. Z. Zhang, T. Hyeon, *J. Am. Chem. Soc.* **2003**, *125*, 11100.
[30] W. Du, X. Qian, J. Yin, Q. Gong, *Chem. Eur. J.* **2007**, *13*, 8840.
[31] D. S. Wang, T. Xie, Q. Peng, Y. D. Li, *Chem. Eur. J.* **2008**, *14*, 2507.
[32] D. S. Wang, T. Xie, Q. Peng, Y. D. Li, *J. Am. Chem. Soc.* **2008**, *130*, 4016.
[33] D. S. Wang, C. H. Hao, W. Zheng, Q. Peng, T. H. Wang, Z. M. Liao, D. P. Yu, Y. D. Li, *Adv. Mater.* **2008**, *20*, 2628.
[34] D. S. Wang, W. Zheng, C. H. Hao, Q. Peng, Y. D. Li, *Chem. Commun.* **2008**, 2556.
[35] C. Sombuthawee, S. B. Bansall, F. A. Hummel, *J. Solid State Chem.* **1978**, *25*, 391.
[36] F. Bai, D. S. Wang, Z. Y. Huo, W. Chen, L. P. Liu, X. Liang, C. Chen, X. Wang, Q. Peng, Y. D. Li, *Angew. Chem.* **2007**, *119*, 6770; *Angew. Chem. Int. Ed.* **2007**, *46*, 6650.

Received: September 3, 2008
Revised: November 26, 2008
Published online: January 2, 2009

